Journal of Structural Geology 31 (2009) 1586–1596

Contents lists available at ScienceDirect

Journal of Structural Geology

journal homepage: www.elsevier.com/locate/jsg

Factors affecting finite strain estimation in low-grade, low-strain clastic rocks

Daniel Pastor-Galán [a,*], Gabriel Gutiérrez-Alonso [a], Patrick A. Meere [b], Kieran F. Mulchrone [c]

[a] Departamento de Geología, Universidad de Salamanca, 37008 Salamanca, Spain
[b] Department of Geology, National University of Ireland, Cork, Ireland
[c] Department of Applied Mathematics, National University of Ireland, Cork, Ireland

ARTICLE INFO

Article history:
Received 17 December 2008
Received in revised form
9 July 2009
Accepted 9 August 2009
Available online 14 August 2009

Keywords:
Strain analysis
Talas Ala Tau
Cantabrian Zone
Mean radial length
SAPE
DTNNM

ABSTRACT

The computer strain analysis methods SAPE, MRL and DTNNM have permitted the characterization of finite strain in two different regions with contrasting geodynamic scenarios; (1) the Talas Ala Tau (Tien Shan, Kyrgyzs Republic) and (2) the Somiedo Nappe and Narcea Antiform (Cantabrian to West Asturian-Leonese Zone boundary, Variscan Belt, NW of Iberia). The performed analyses have revealed low-strain values and the regional strain trend in both studied areas. This study also investigates the relationship between lithology (grain size and percentage of matrix) and strain estimates the two methodologies used. The results show that these methods are comparable and the absence of significant finite strain lithological control in rocks deformed under low metamorphic and low-strain conditions.

1. Introduction

Strain determination using populations of deformed objects is a useful technique for understanding the processes and products of deformation of the Earth's crust from the micro- to macro-scales (Mulchrone et al., 2005). Ramsay (1967) came up with the idea of measuring finite strain from randomly oriented populations of deformed objects, the so-called the $R_f/\emptyset$ method for strain analysis. Subsequently, alternative methods, using different objects or relationships among them, have been developed (Dunnet, 1969; Elliott, 1970; Dunnet and Siddans, 1971; Matthews et al., 1974; Borradaile, 1976; Shimamoto and Ikeda, 1976; Robin, 1977; Lisle, 1977a,b, 1985; Peach and Lisle, 1979; Yu and Zheng, 1984; Mulchrone and Meere, 2001; Mulchrone et al., 2003).

An alternative strain analysis methodology is based on object–object separation (Ramsay, 1967). This original method, known as the Fry method (1979), was subsequently further developed as the Normalised Fry Method (Erslev, 1988) and the enhanced Normalised Fry Method (Erslev and Ge, 1990). More recently further insights into the object separation techniques have allowed McNaught (1994) to extend these methods in order to avoid the problems associated with approximating non-elliptical grains by best-fit ellipses. Mulchrone (2002) showed that the application of Delaunay triangulation to the determination of nearest object separations, was a faster and less subjective strain determination technique.

All these aforementioned methods rely on the assumption that the ellipsoidal markers (generally rock grains) act passively during the rock deformation process. Nevertheless, if matrix-supported sedimentary clasts are used as strain markers, the competence contrast between the clasts and the matrix can be significant. To avoid this problem (Treagus and Treagus, 2002) combined $R_f/\emptyset$ techniques (Ramsay, 1967; Dunnet, 1969; Robin, 1977) characterizing strain based on clast shape with centre-to-centre methods (Fry, 1979; Erslev, 1988; Erslev and Ge, 1990; Mulchrone, 2002) in order to characterize bulk rock strain. Moreover, Meere et al. (2008) illustrated that it is possible to significantly underestimate the strain in rocks deformed under low-grade conditions when this assumption is not valid, even when using centre-to-centre methods.

An additional concern is that the percentage of matrix and the concentration and packing style of grains can have significantly influence on finite strain estimates from multi-phase deformed rocks (Gay, 1968; Lisle, 1979). Mandal et al. (2003) showed that high object concentrations led to reduced strain partitioning (which is the ratio between object and bulk strain values). Vitale and Mazzoli (2005) noted that high concentrations of ooids in packstones resulted in a significant underestimation of the bulk strain and the object strain.

Here we present analyses of the finite strain measured in 84 rock samples, each with varying percentages of matrix, and different

* Corresponding author.
E-mail address: dpastorgalan@usal.es (D. Pastor-Galán).

0191-8141/$ – see front matter © 2009 Elsevier Ltd. All rights reserved.
doi:10.1016/j.jsg.2009.08.005

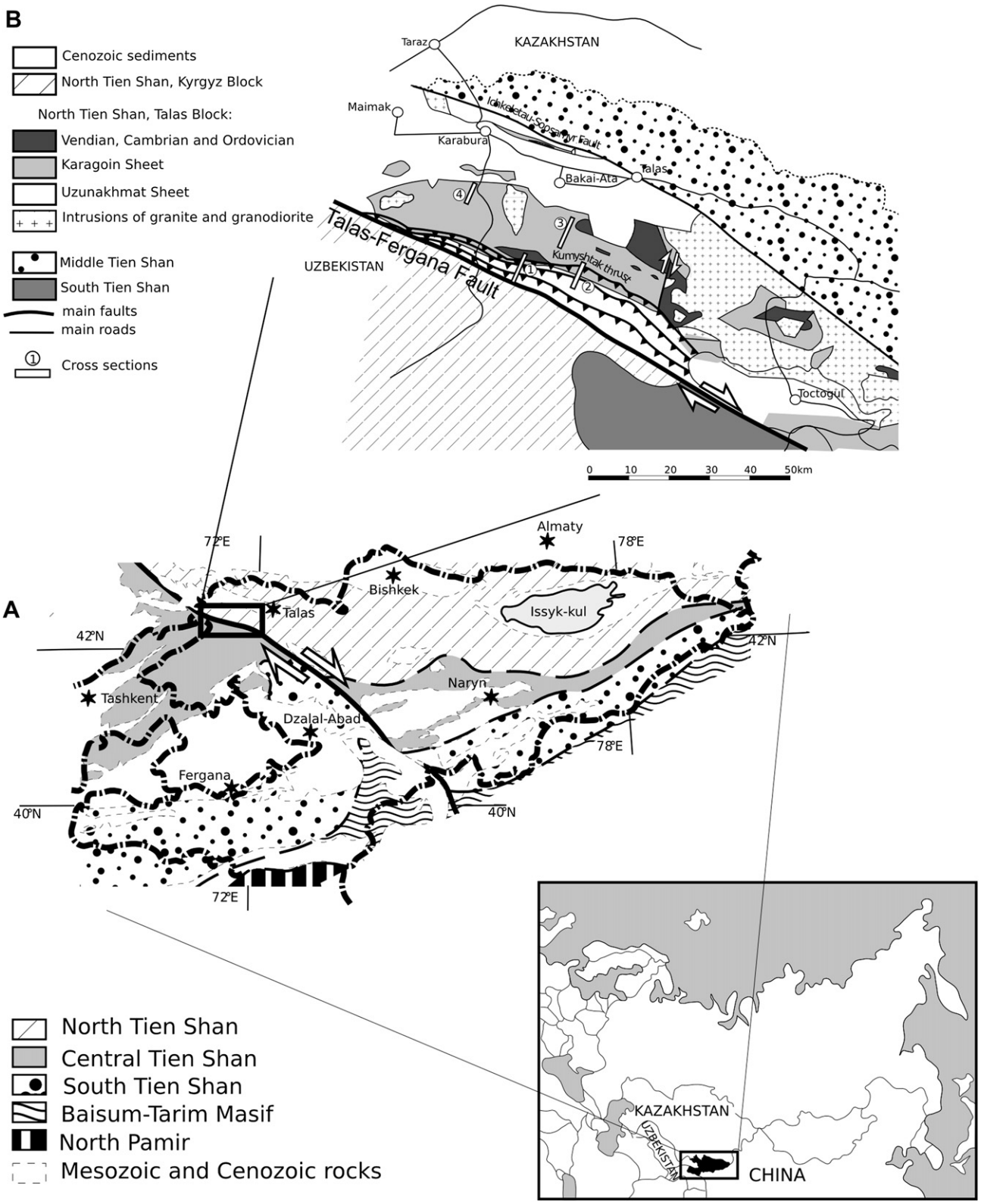

Fig. 1. (A) Geographical location of the main geological Tien Shan Belt domains in the Kyrgyz Republic. (B) General geological map of Talas Ala Tau (after Abad et al., 2003), indicating the location of the detailed cross-sections where studied samples were picked up: (1) Postunbulak; (2) Beskol; (3) Urmaral; (4) Karabura.

object concentrations. These rocks were deformed under low finite strain regimes and very low metamorphic grade conditions in two distinct geodynamical environments. The strain analyses were performed with three standardized methods: the mean radial length method (Mulchrone et al., 2003), Normalised Fry Method and DTNNM (Mulchrone, 2002).

In this paper, we characterize statistically the sort of population of finite strain results obtained in both studied areas and determine

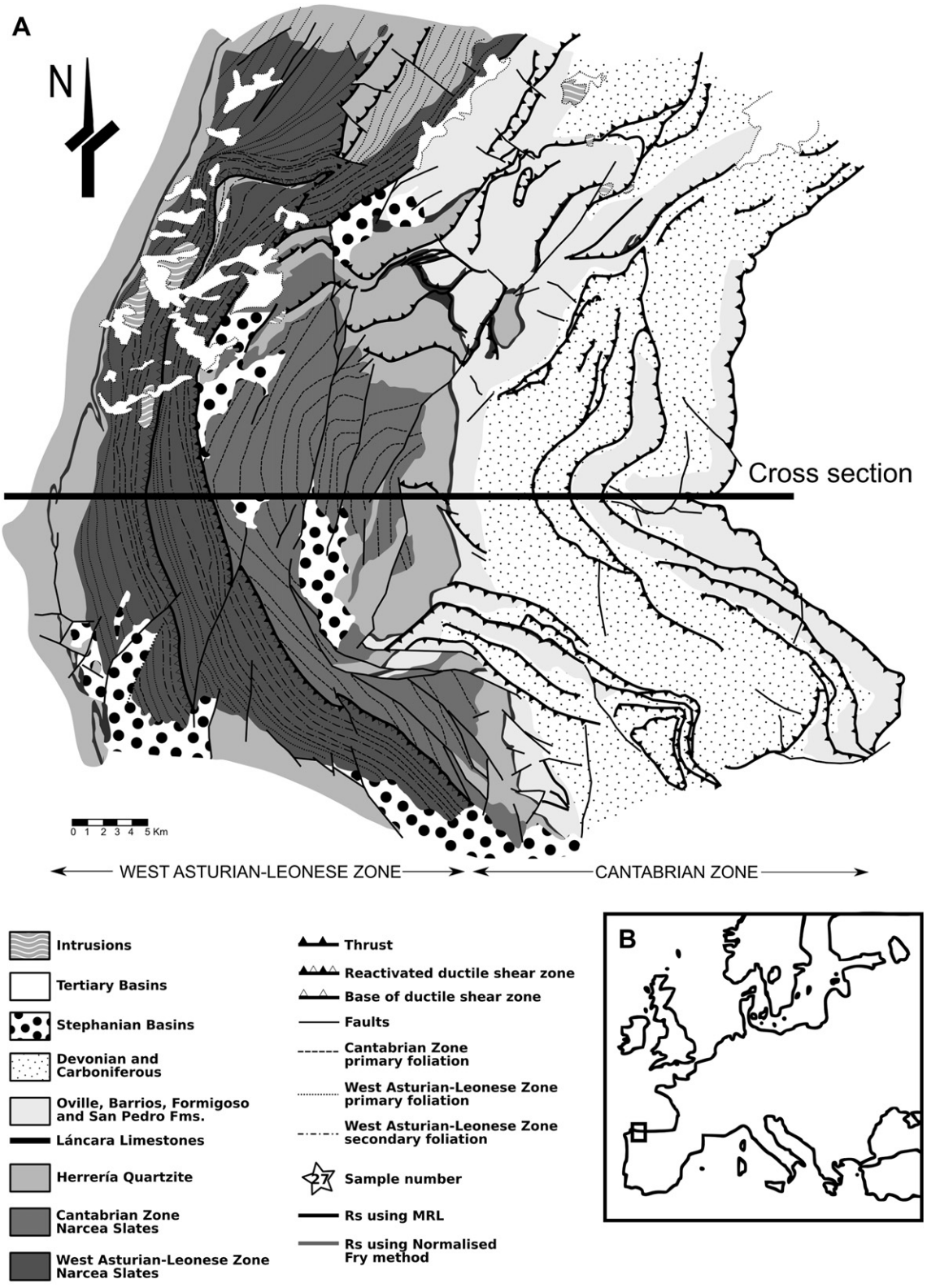

Fig. 2. A) Geological map of the Narcea Antiform and Somiedo Nappe after Gutiérrez-Alonso (1992, 1996). A–A′ trace of the cross-section showed in Fig. 11 (CZ – Cantabrian Zone, WALZ – West Asturian-Leonese Zone). B) Location of the Narcea Antiform and Somiedo Nappe.

if they depict one or more fractal dimension geological features, such as fracture populations (Marret and Allmendiger, 1991, 1992) and folds (Wu, 1993), can be described as fractals. There are two basic types of fractals: self-similar and self-affine (Mandelbrot, 1967, 1983, 1985). A self-similar fractal has a universal self-similarity which does not change with scale. Self-affine fractals have a non-isotropic similarity (Mandelbrot, 1985; Wu, 1993). The fractal dimension is a property of a fractal population or of an object and

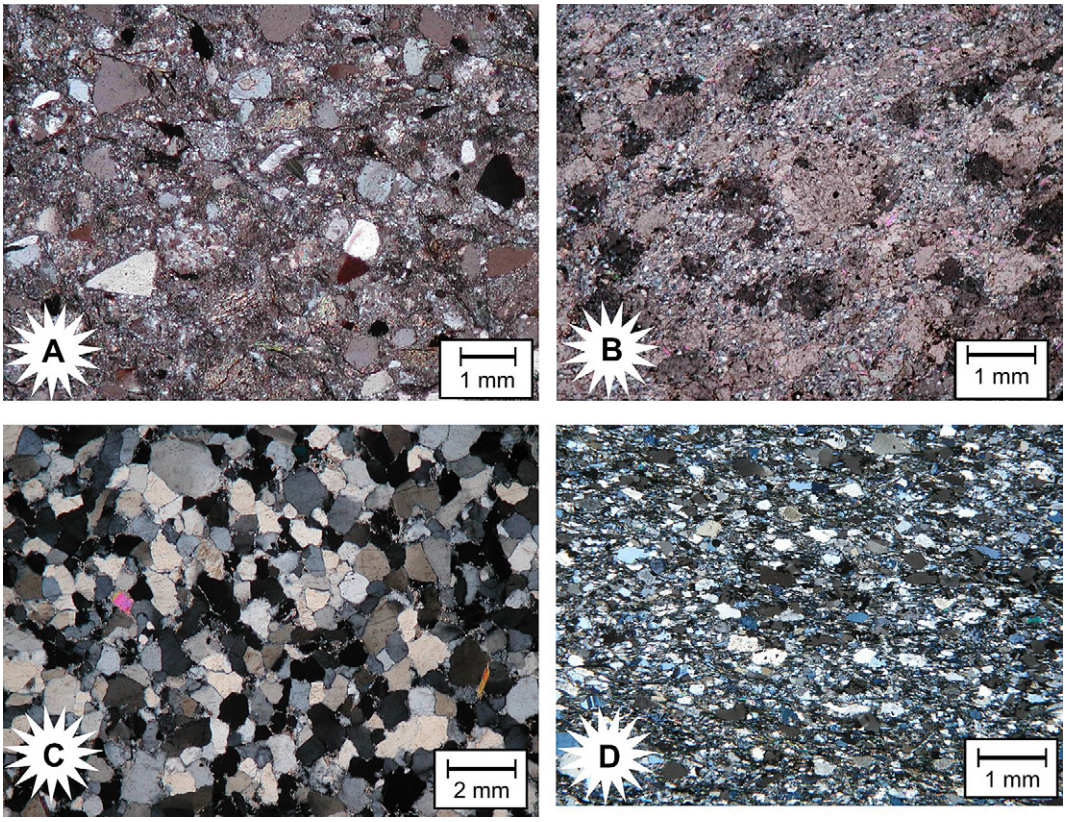

Fig. 3. (A) Microphotograph of a Talas Ala Tau greywacke. (B) Microphotograph of a fine grain Talas Ala Tau greywacke with carbonate cement. (C) Microphotograph of the Barrios formation in the Somiedo Nappe. (D) Microphotograph of the Narcea Slates in the West Asturian-Leonese Zone side of the Narcea Antiform.

can be an integer, in which case it is equivalent to the Euclidean dimension of the population or object. The Euclidean dimension of a point is zero, of a line segment is one etc., but in general terms fractal dimension is not an integer but a fractional dimension (Turcotte, 1992). In geology, it is usually interpreted that different fractal dimensions in one population might indicate different formation processes.

Samples for strain analysis in this study are greywackes and sandstones with varying proportions of matrix that were collected from the Talas Ala Tau fold-and-thrust belt of the Tien Shan, Kyrgyz Republic; and the Narcea Antiform and Somiedo Nappe in the Cantabrian Zone, located in the Variscan Belt in NW Iberia. These two thrusts belts are characterized by similar structures, alike strain regimes and very low metamorphic grade, but were developed under two different geodynamic scenarios making them good candidates for comparing results raising from different processes.

The Tien Shan range was uplifted during Cenozoic collision between India and Eurasia. The subsequent erosion of these mountains has exposed rocks deformed during previous orogenic events that were responsible for the building and amalgamation of western Asia (Abdrakhmatov et al., 1996; Bullen et al., 2001; Abad et al., 2003). The Tien Shan mountain range is usually divided into North, Central and South Tien Shan zones (Fig. 1A).

As South and Central Tien Shan deformation is only due to the Uralian orogeny, in the North Tien Shan, where the Talas Ala Tau is located, a Cadomian–Baikalian deformation event can also be recognized (Kiselev et al., 1988; Allen et al., 2001). This Cadomian–Baikalian orogeny is interpreted as being responsible for the main shortening event, involving the formation of thrusts and folds, and for the widespread development of a penetrative to non-penetrative axial planar cleavage.

The rocks of the Talas Ala Tau are mostly sedimentary rocks of Cryogenian to Ediacaran age (Korolev and Maksumova, 1980; Kiselev and Korolev, 1981). They crop out in two different thrust sheets (or domains), separated by km scale thrusts, known as Uzunakhmat (SW) and Karagoin (NE) sheets (Fig. 1B). The main

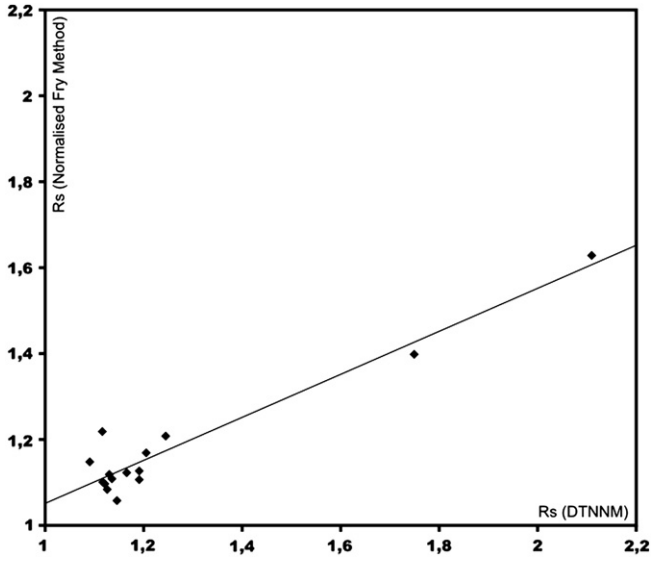

Fig. 4. Plot of the strain measured with DTNNM versus Normalised Fry Method in the samples with very low or no matrix content, where DTNNM works correctly. Normalised Fry Method shows a little R_s underestimation. Linear regression is used, showing an R^2 of 0.92.

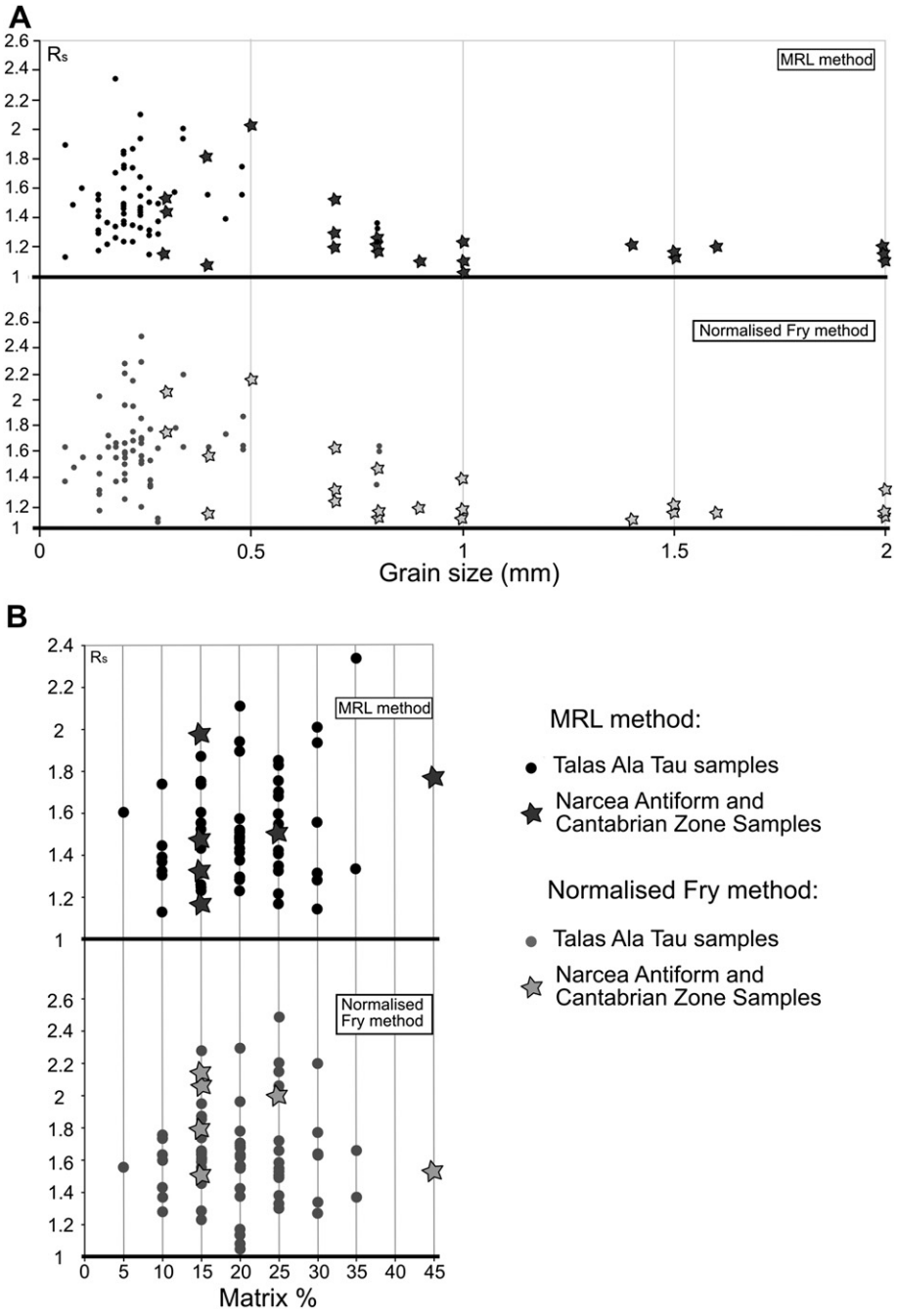

Fig. 5. (A) Plot of mean grain size and strain measured (R_s) with both MRL and Normalised Fry Methods. (B) Plot of % of matrix versus strain measured (R_s) with both methods.

thrust that separates the domains is the Kumyshtak thrust, which is estimated to have accommodated more than 10 km of reverse displacement (Abad et al., 2003). The southern limit of the Talas Ala Tau is the Talas-Fergana fault (Burtman et al., 1996), a long-lived dextral strike–slip fault with a displacement greater than 220 km and a complex history.

Ordovician limestones overlie the two thrust sheets along an angular unconformity, suggesting that the Precambrian strata were involved in a Precambrian or Cambrian deformation event. The Paleozoic rocks were subsequently folded during Uralian orogeny and were intruded by granite plutons at that time. Moreover the Himalayan orogeny uplifted, rotated and tilted all previous structures.

The metamorphic evolution of the Talas Ala Tau was studied using the phyllosilicates related to the Cadomian–Baikalian cleavage by Abad et al. (2003), after Forlova (1982), indicates that the metamorphic grade in the Uzunakhmat sheet increases to the south reaching greenschists facies while the Karagoin sheet is not metamorphosed. Their results show a high pressure (at least 8 kbar)/low temperature (below 300 °C) metamorphism in the Uzunakhmat sheet, which suggests a subduction related geodynamic environment to explain the deformation.

There are two preliminary strain data sets from this region; Khudoley (1993) studied a limited set of samples using the Fry and $R_f/\emptyset$ methods with the strain ratio (R_s) results ranging between 1.2 and 6.2. More recently Voitenko et al. (2004) have obtained R_s

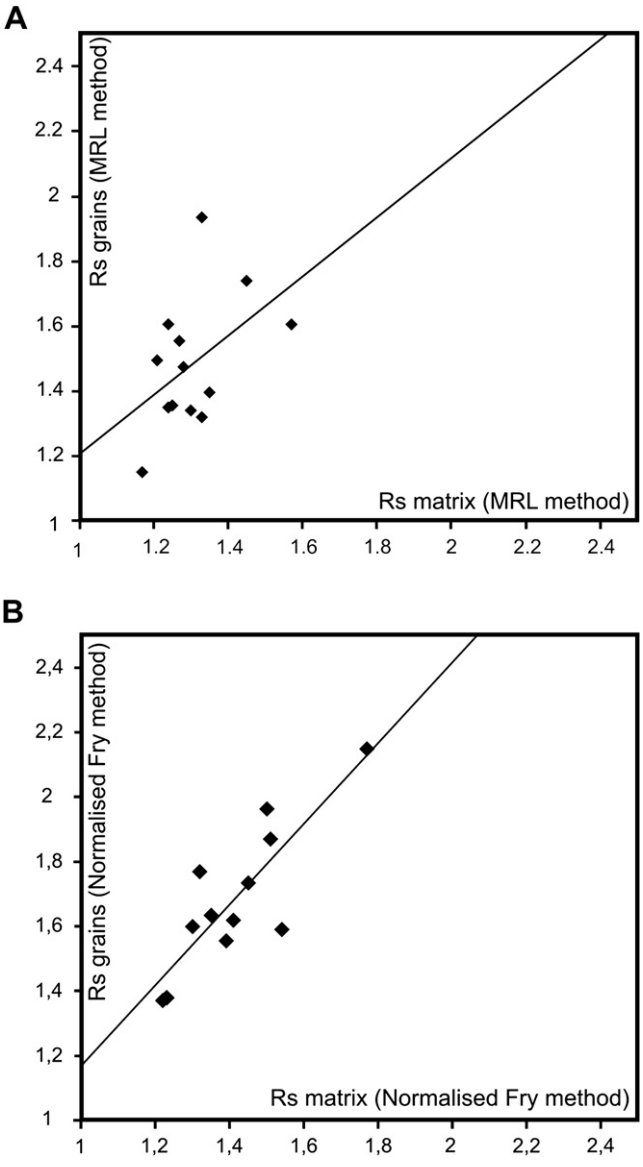

Fig. 6. (A) Plot of the strain measured (R_s) in very fine quartz grains (matrix) and R_s measured in grains with MRL. (B) Plot of the strain measured in the matrix and R_s measured in grains with Normalised Fry Method. Linear regression is used.

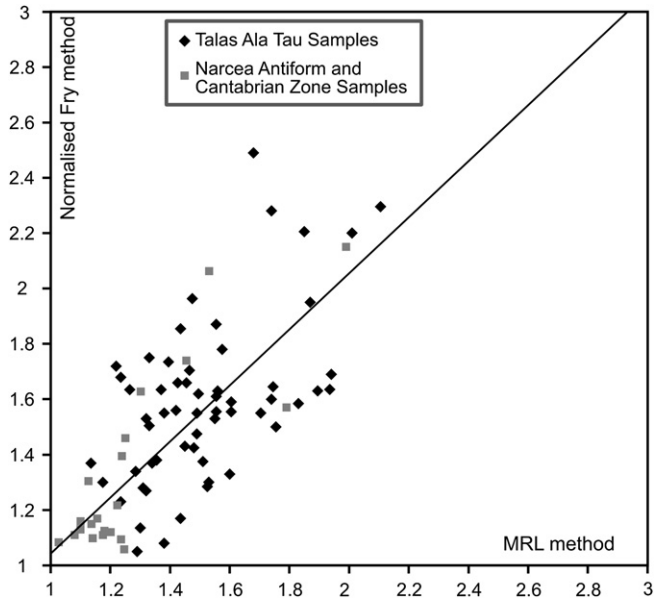

Fig. 7. Plot of the R_s obtained using MRL versus using Normalised Fry Method. This plot shows an insignificant underestimation of strain using the MRL method. Best-fit line drawn was obtained by linear regression. Five anomalous values were not considered for the linear regression analysis.

results which vary between 1.1 and 2 using the enhanced Normalised Fry Method.

The Narcea Antiform and Somiedo Nappe are neighbouring units situated in the Variscan Orogen of northwestern Iberia. The regional structural trend describes an arcuate shape whose origin is interpreted as an orocline (Weil et al., 2000, 2001; Gutiérrez-Alonso et al., 2004). The Narcea Antiform (Julivert, 1971; Gutiérrez-Alonso, 1996) is an asymmetric foreland-verging fold that straddles the limit between the foreland Cantabrian Zone, and the hinterland Western Asturian-Leonese Zone (Fig. 2).

The western hinterland flank of the Narcea Antiform records three stages of deformation (Gutiérrez-Alonso, 1992; Díaz-García, 2006). However, the eastern foreland limb of the antiform, is less deformed and metamorphosed than the western side and only shows the development of a cleavage fabric. The La Espina thrust, which is a ductile thrust, separates the east and west limbs, and defines the limit between the hinterland and foreland (Gutiérrez-Alonso, 1987, 1992, 1996, 2004). Strain analysis and metamorphic studies (Gutierrez-Alonso and Nieto, 1996; Gutiérrez-Alonso, 1996) indicate very low to low-grade metamorphic conditions (never reaching the epizone) and R_s values from 1 to 3.

The Somiedo Nappe is the westernmost large allochthonous unit situated in the Cantabrian Zone. Cleavage is only locally developed or is not present at all. A very low grade of metamorphism is indicated by illite crystallinity and CAI (conodont colour alteration index) studies, in the western and northwestern area of the Cantabrian Zone (García López et al., 2007 and references therein).

The rocks from Talas Ala Tau are mainly poorly sorted greywackes and sandstones with high matrix content (between 5 and 40%) and irregular clasts. Some of the studied samples have abundant carbonate cement (Fig. 3B). The most frequent rocks in the Narcea Antiform are the Upper Proterozoic slates and greywackes. Somiedo Nappe rocks are mainly well sorted sandstones and quartzites with little or no matrix (Fig. 3C).

2. Methods

To quantify the strain recorded by the rocks in this study we have used two different strain analysis techniques: (1) the mean radial length (Mulchrone et al., 2003), to characterize the clast strain and (2) the Delaunay Triangulation Nearest Neighbour Method (DTNNM) (Mulchrone, 2002), which has been used as an intermediary for the Normalised Fry Method (Erslev, 1988) as well as a control method to measure the bulk finite strain. The parameters needed to perform the strain analysis were extracted from microphotographs using the semiautomatic parameter extraction software (SAPE) developed by Mulchrone et al. (2005). At least 150 clasts were selected for each microphotograph, as per the recommendation of Meere and Mulchrone (2003). Two or three microphotographs, each from a different portion of each thin section, were analysed in order to minimize the observational biases and errors. For this study, 84 thin polished sections were cut normal to the fold axis (normal to the S_0/S_1 intersecting lineation). In 13

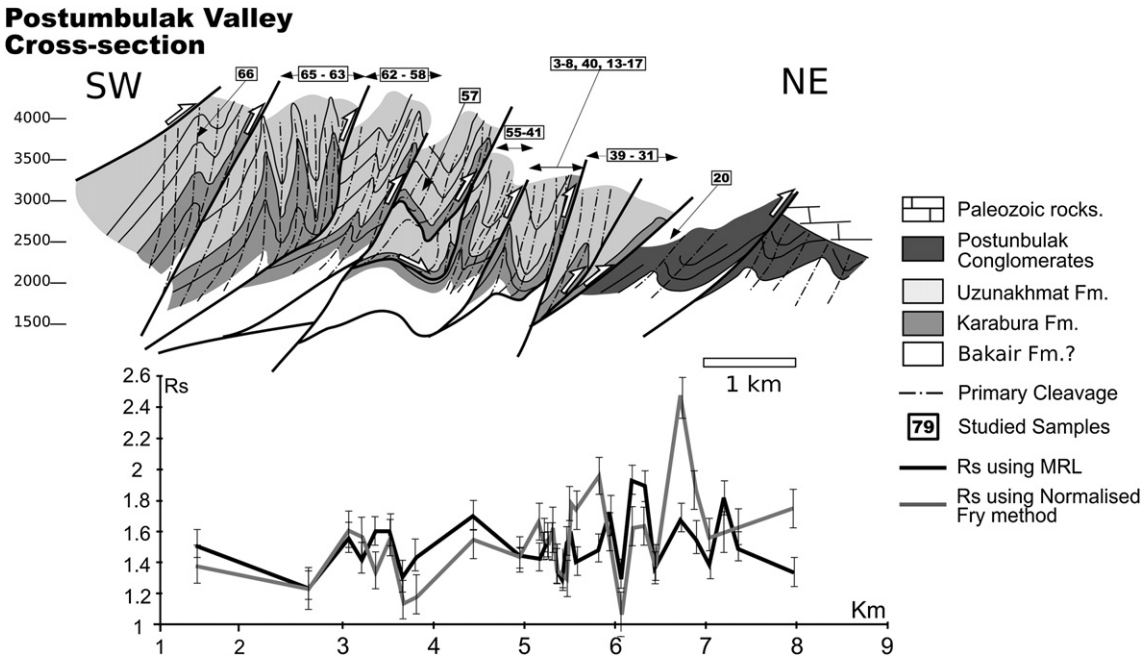

Fig. 8. Postunbulak valley cross-section (Uzunakhmat sheet) after Abad et al. (2003). Below it the strain variations along the cross-section are plotted both MRL and Normalised Fry Method with the 95% confidence interval bars included. Location of samples studied is showed.

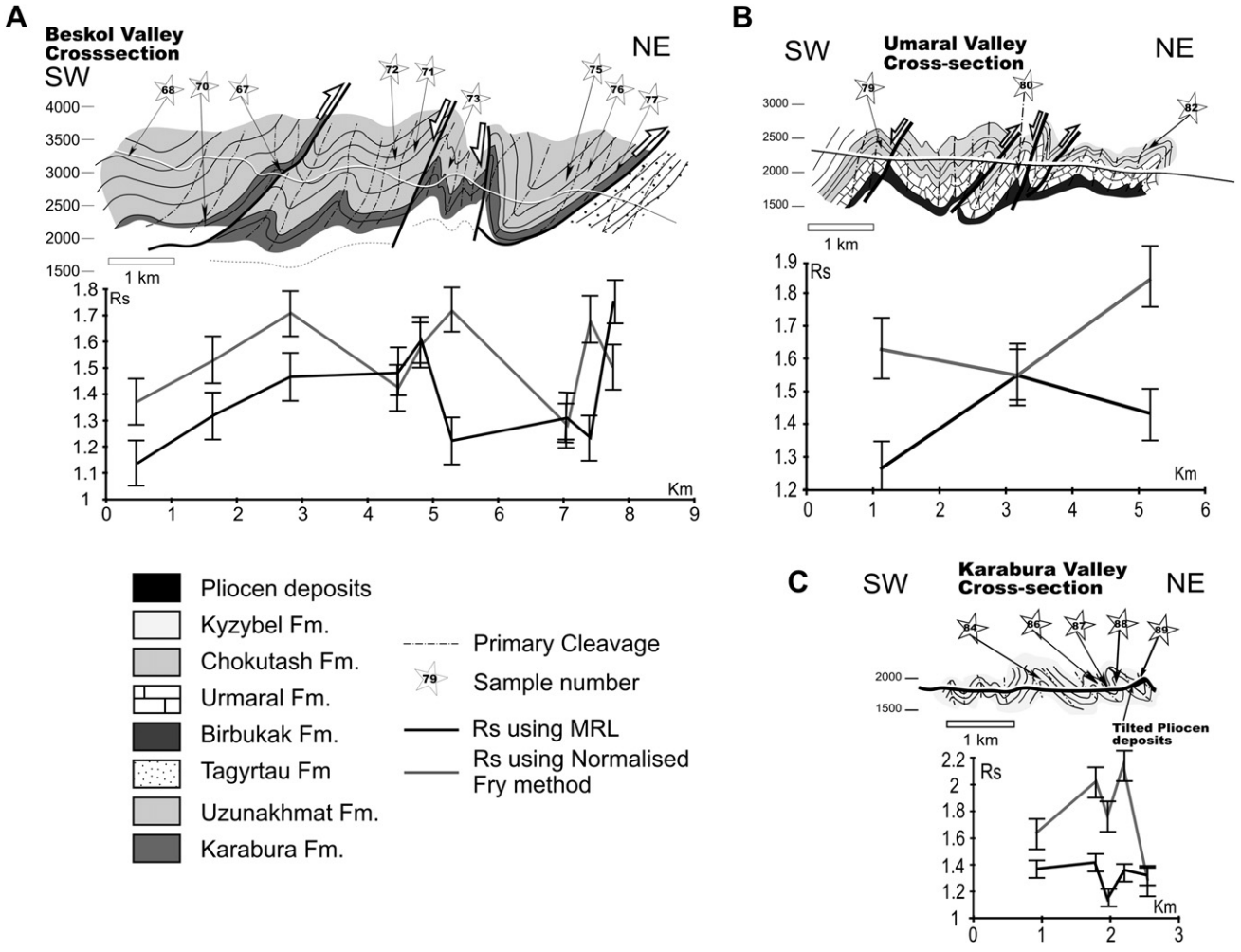

Fig. 9. (A) Beskol valley cross-section (Uzunakhmat sheet) after Abad et al. (2003) with the strain variations measured with MRL and Normalised Fry Method below it. (B) Urmaral valley cross-section (Karagoin sheet) after Abad et al. (2003) showing the strain variations measured with both methods employed. (C) Karabura Valley cross-section (Karagoin sheet) after Abad et al. (2003) below the cross-section strain variations measured with MRL and Normalised Fry Method are plotted. All of them show the 95% confidence interval bars and the location of the samples studied.

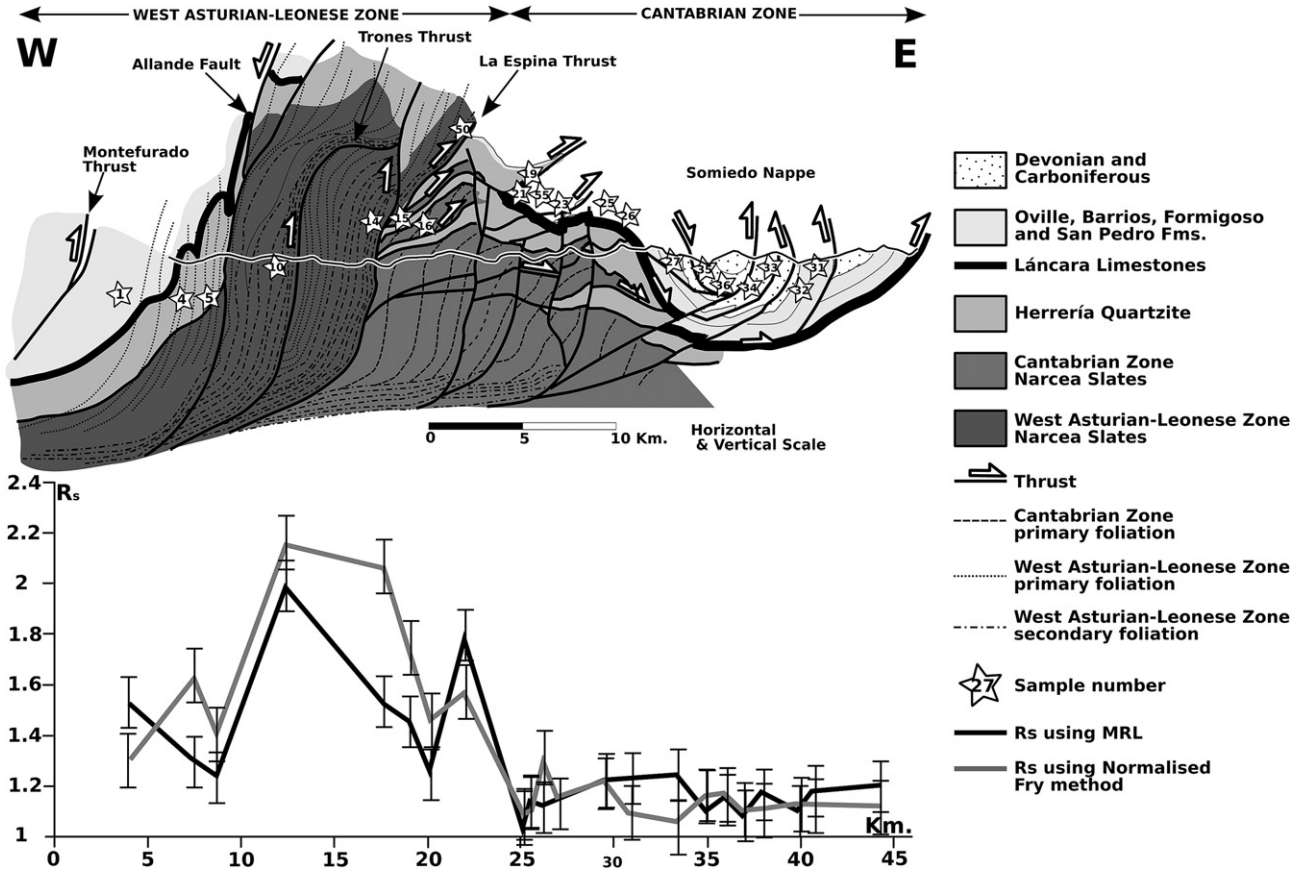

Fig. 10. Narcea Antiform and Somiedo Nappe cross-section after Gutiérrez-Alonso (1992, 1996). Below it the plot showing variations of the strain measured with MRL and Normalised Fry Method is depicted. 95% confidence bars are shown.

samples finite strain in very fine quartz grains from the matrix were also selected and analysed.

The mean radial length (MRL) (Mulchrone et al., 2003) is used to calculate the finite strain from the shape and orientation of objects. This method is based on the conceptually simple fact that the mean radial length of a set of randomly oriented ellipses in the unstrained state averages to a circle, so that after strain the mean radial length equates to the strain ellipse. It has been demonstrated that error bars associated with the MRL method are smaller than those of other methods (Mulchrone, 2002, 2005).

The DTNNM (Mulchrone, 2002) has been used to measure the bulk strain using the spacing between objects. DTNNM put into practice the Delaunnay triangulation in order to simplify the uses of the Ramsay's Nearest Neighbour Method. However, DTNNM has to be used cautiously with loosely packed rocks (Mulchrone, 2002, 2005). For this reason DTNNM has been used in this study, due to the characteristics of the Talas Ala Tau rocks which are typically poorly sorted greywackes with a large percentage of matrix, as an intermediary for the Normalised Fry Method (Erslev, 1988) obtaining from DTNNM the scatterplot and estimating the strain ellipse graphically.

3. Results

The large percentage of matrix in many of the samples hindered the use of the DTNNM. Fig. 4 compares the estimation of strain through DTNMM against Normalised Fry Method in the samples where DTNNM works correctly showing a R^2 correlation of 0.92 and a little underestimation of R_s using the Normalised Fry Method. In order to test the possible correlation between the percentage of matrix (A) and average clast size (B) versus R_s we constructed plots

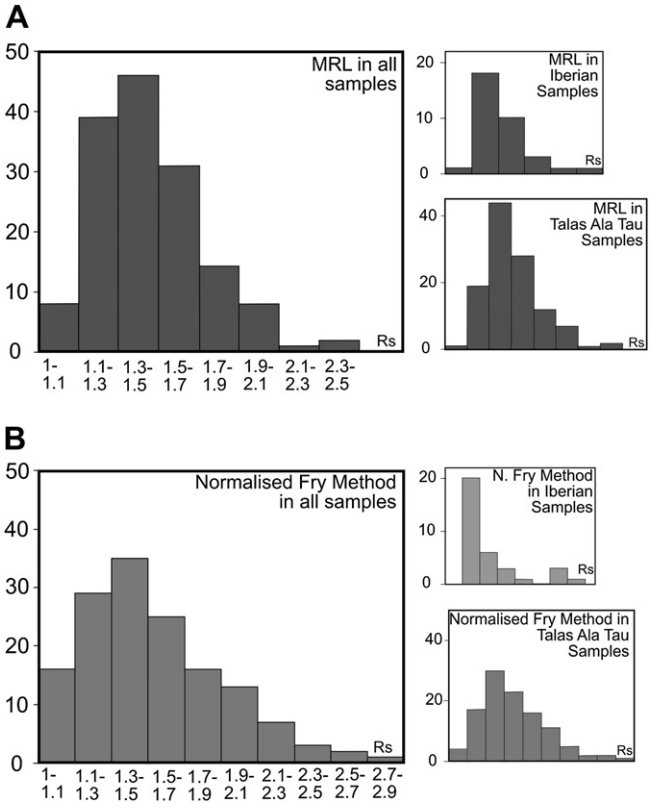

Fig. 11. Plots of population of strain both in Talas Ala Tau, Narcea Antiform and Somiedo Nappe (Iberian samples) and all samples together measured with MRL (A) and Normalised Fry Method (B).

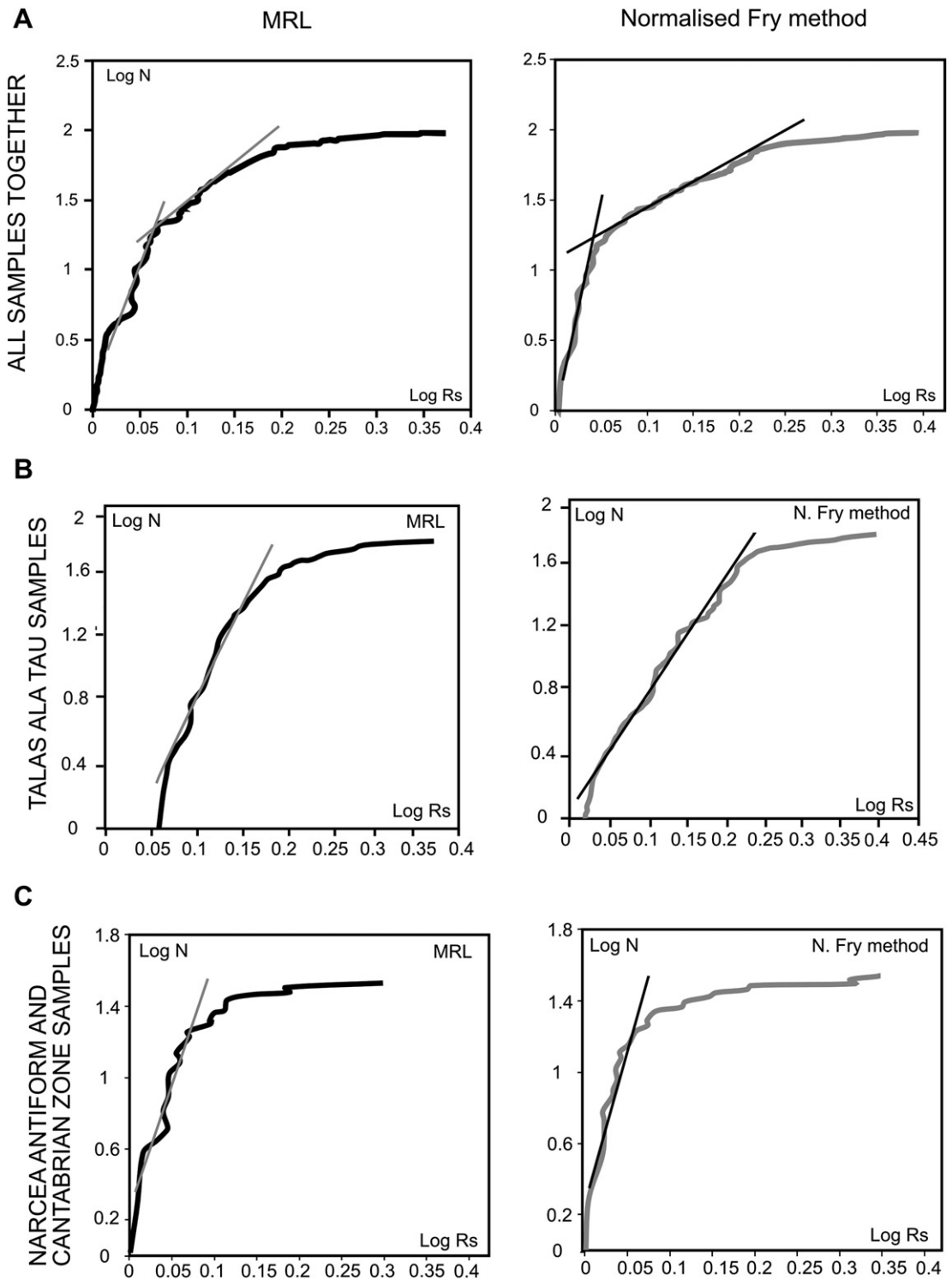

Fig. 12. Plot of fractal analysis with both methods employed showing all samples together (A), Talas Ala Tau samples (B) and Narcea Antiform and Somiedo Nappe samples (Iberian samples) (C). Straight lines show fractal populations.

of clast size and percentage of matrix against strain (Fig. 5). From these plots it might be interpreted that the larger grain sizes yield lower R_s estimates. This is, however, an artefact of the sampling; the samples with large grain size all come from Somiedo Nappe where both large grain size rocks and fine grain samples are unstrained as is expected in a typical foreland thrusts and fold belt. There is, therefore, no observable correlation between grain size or percentage of matrix and strain. Fig. 6 exhibits the relationship between the strain measured in the matrix against the R_s obtained in the grains, matrix shows shorter R_s values than the recorded by the grains. Normalised Fry method vs. MRL method plot of the results obtained in this study yields a good, albeit not optimal correlation showing a little underestimation of strain using MRL showing a very little underestimation of strain using MRL (Fig. 7).

The finite strain data obtained from the studied samples were plotted along the studied cross-sections (Figs. 8 and 9) (Pastor-Galán, 2008; Pastor-Galán et al., 2008a,b). Significant variations in the regional finite strain were found along section in both areas. In Talas Ala Tau, R_s values range between 1.1 and 2.6, and increase toward the thrust surfaces. Increased strain adjacent to the thrust faults is interpreted to be caused by the local increase of simple shear near the faults (Abad et al., 2003). R_s values vary between 1.1 and 2.1 across the Narcea Antiform and Somiedo Nappe (Fig. 10). R_s is highest in the western flank of the Narcea Antiform, probably due to presence of large regional shear zones (Gutiérrez-Alonso, 1996) including the Trones and La Espina thrusts (Fig. 10). R_s is very low and homogenous without any observable variation across the Somiedo Nappe. These results are the expected ones since they are consistent with field observations.

The plot of population analysis (Fig. 11) shows that the studied samples behave as log-normal populations, both individually and when considered collectively. Our fractal analysis (Fig. 12), employing the method described by Turcotte (1992), shows that finite strain behaves in a self-similar way as do fracture populations and earthquakes. This implies that it is not necessary to have very large data sets to produce significant and meaningful results. The representative segments in these plots are the central portions; the left and right segments represent the under-sampled upper and lower limits, respectively, as proposed by Marret and Allmendiger (1991, 1992). As expected, when the Talas Ala Tau and Variscan populations are considered together they describe two different distributions; when plotted independently they are unique. These results may indicate that different mechanisms, perhaps due to the differing geodynamic settings of the two regions, were responsible for imparting the strain onto these rocks.

4. Conclusions

The literature usually assumes high percentage matrix rocks deformed under low metamorphic conditions and low-strain rates accumulate deformation on matrix while grains don't change shape nor orientation. Because of this reason it is generally supposed centre-to-centre methods are closer to the real strain values than $R_f/\emptyset$ methods, which don't produce acceptable results. Using both methods, in samples from the Talas Ala Tau and the Narcea Antiform and Somiedo Nappe, we find no correlation between the measured finite strain and either grain size or the percentage of matrix (Fig. 5). With the obtained results, we conclude that neither grain size or percentage of matrix controls strain recorded by this kind of clastic rocks in low-grade regimes. Furthermore, the matrix records the same R_s ratio as the whole rock (Fig. 6). Therefore the matrix ratio, or object concentration, and grain size of a rock is not a restriction in finite strain analyses for low-grade clastic rocks. We support that rocks similar to the described in this work behave passively under low metamorphic grade and low-strain conditions, even if the rocks present a considerable competency contrast between clasts and matrix.

Moreover, the results from the MRL and Normalised Fry Methods yielded similar values, and indicate that the two methods provide comparable results for clastic rocks deformed under low-strain rates independently of the grain size or matrix ratio. In addition, the validity of the use of DTNNM as an intermediary method for the Normalised Fry Method has been confirmed (Mulchrone, 2002, 2005) as it yields comparable results (Fig. 4).

The strain populations in the two studied fold-and-thrust belts yield unique log-normal distributions. It is to be expected that every population rocks of low finite strain will be log-normal. However, fractal analysis distinguishes independent populations in the two different areas, possibly reflecting the different mechanisms and differing geodynamic settings responsible for deformation within the two study areas.

Acknowledgments

Critical and constructive reviews by Richard Lisle and an anonymous reviewer have helped to improve the manuscript. Financial support was supplied by Research Project ODRE ("Oroclinales Delaminación Relaciones y Efectos") No. CGL2006-00902, from the Spanish Ministry of Science and Innovation and an ACPI grant from the Junta de Castilla y León.

References

Abad, I., Gutiérrez-Alonso, G., Nieto, F., Gertner, I., Becker, A., Cabero, A., 2003. The structure and the phyllosilicates (chemistry, crystallinity and texture) of Talas Ala-Tau (Tien Shan, Kyrgyz Republic): comparison with more recent subduction complexes. Tectonophysics 365, 103–127.

Abdrakhmatov, K.Y., Aldazhanov, S.A., Hager, B.H., Hamburger, M.W., Herring, T.A., Kalaev, K.B., Makarov, V.I., Molnar, P., Panasyuk, S.V., Prilepin, M.T., Reilinger, R.E., Sadybakasov, I.S., Souter, B.J., Trapeznikov, Y.A., Tsurkov, V.Y., Subobich, A.V., 1996. Relative recent construction of the Tien Shan inferred from GPS measurements of present day crustal deformation rates. Nature 384, 450–453.

Allen, M.B., Alsop, G.I., Zhemchuzhnikov, V.G., 2001. Dome and basin refolding and transpressive inversion along the Karatu fault system, southern Kazakhstan. Journal of the Geological Society (London) 158, 83–95.

Borradaile, G.J., 1976. A study of a granite/granite gneiss transition and accompanying schistosity formation in SE Spain. Journal of the Geological Society (London) 132, 417–428.

Bullen, M.E., Burnak, D.W., Garver, J.L., Abdrakhmatov, K.Y., 2001. Late Cenozoic Evolution of the northwestern Tien Shan: new age estimates for the initiation of mountain building. Geological Society of American Bulletin 113, 1544–1559.

Burtman, V.S., Skobelev, S.F., Molnar, P., 1996. Late Cenozoic slip on the Talas-Fergana fault, the Tien Shan, Central Asia. Geological Society of America Bulletin 108, 1544–1559.

Díaz-García, F., 2006. Geometry and regional significance of Neoproterozoic (Cadomian) structures of the Narcea Antiform, NW Spain. Journal of the Geological Society (London) 163, 499–508.

Dunnet, D., 1969. A technique of finite strain analysis using elliptical particles. Tectonophysics 7, 117–136.

Dunnet, D., Siddans, A.W.B., 1971. Non-random sedimentary fabrics and their modification by strain. Tectonophysics 12, 307–325.

Elliott, D., 1970. Determination of finite strain and initial shape from deformed elliptical objects. Geological Society of America Bulletin 81, 2221–2236.

Erslev, E.A., 1988. Normalized center-to-center strain analysis of packed aggregates. Journal of Structural Geology 10, 201–209.

Erslev, E.A., Ge, H., 1990. Least squares center-to-center and mean object ellipse fabric analysis. Journal of Structural Geology 8, 1047–1059.

Forlova, N.S., 1982. Influence of metamorphism on deformational properties of rocks (an example from Talas Ala Tau). Geotectonika 4, 18–24.

Fry, N., 1979. Random point distributions and strain measurement in rocks. Tectonophysics 60, 806–807.

García López, S., Brime, C., Valín, M.L., Sanz-López, J., Bastida, F., Aller, J., Blanco-Ferrara, S., 2007. Tectonothermal evolution of a foreland fold and thrust belt: the Cantabrian Zone (Iberian Variscan belt, NW Spain). Terra Nova 19, 469–475.

Gay, N.C., 1968. Pure shear and simple shear deformation of inhomogeneous viscous fluids. 1. Theory. Tectonophysics 5, 211–234.

Gutiérrez-Alonso, G., 1987. La estructura de la parte Norte de la ventana tectónica del Narcea. Seminario de Investigación, Oviedo University.

Gutiérrez-Alonso, G., 1992. El Antiforme del Narcea y su relación con los mantos occidentales de la Zona Cantábrica. PhD thesis, Oviedo University.

Gutiérrez-Alonso, G., 1996. Strain partitioning in the footwall of the Somiedo Nappe: structural evolution of the Narcea Tectonic Window. Journal of Structural Geology 10, 1217–1230.

Gutiérrez-Alonso, G., 2004. La transición de la Zona Asturoccidental-Leonesa con la Zona Cantábrica: el Antiforme del Narcea. In: Vera, J.A. (Ed.), Geología de España. SGE-IGME, Madrid, pp. 52–54.

Gutiérrez-Alonso, G., Fernández-Suárez, J., Weil, A.B., 2004. Orocline triggered lithospheric delamination. In: Weil, A.B., Sussman, A. (Eds.), Paleomagnetic and Structural Analysis of Orogenic Curvature. Special Paper 383. Geological Society of America, Boulder, pp. 121–131.

Gutierrez-Alonso, G., Nieto, F., 1996. White mica crystallinity, finite strain and cleavage development across a large Variscan structure, NW Spain. Journal of Structural Geology 153, 287–299.

Julivert, M., 1971. Décollement tectonics in the Hercynian Cordillera of NW Spain. American Journal of Science 270, 1–29.

Khudoley, A.K., 1993. Structural and strain analyses of the middle part of the Talassian-Alatau ridge (Middle Asia, Kirgizstan). Journal of Structural Geology 15 (6), 693–706.

Kiselev, V.V., Apayarov, F.H., Becker, A., 1988. The Epibaicalic Precambrian of Tien Shan. Ilim, Frunze, pp. 127–143. (in Russian).
Kiselev, V.V., Korolev, V.G., 1981. Paleotectonics of the Tien Shan Precambrian and Lower Paleozoic. Ilim, Frunze, p. 60. (in Russian).
Korolev, V.G., Maksumova, R.A., 1980. Flysch association of the upper Riphean of the Talas Range. International Geology Review 22 (3), 349–360.
Lisle, R.J., 1977a. Estimation of the tectonic strain ratio from the mean shape of deformed elliptical markers. Geologie en Mijnbouw 56, 140–144.
Lisle, R.J., 1977b. Clastic grain shape and orientation in relation to cleavage from the Aberystwyth Grits, Wales. Tectonophysics 39, 381–395.
Lisle, R.J., 1979. Strain analysis using deformed pebbles: the influence the initial pebble shape. Tectonophysics 60, 263–277.
Lisle, R.J., 1985. Geological Strain Analysis: a Manual for the $R_f/ø$ Technique. Pergamon Press, Oxford.
Mandal, N., Samanta, S.K., Bhattacharyya, G., Chakraborty, C., 2003. Deformation of ductile inclusions in a multiple inclusion system in pure and simple shear. Journal of Structural Geology 25, 209–221.
Mandelbrot, B.B., 1967. How long is the coast of Britain? Statistical self-similarity and fractional dimension. Science 156, 636–638.
Mandelbrot, B.B., 1983. In: The Fractal Geometry of Nature. W.H. Freeman, New York.
Mandelbrot, B.B., 1985. Self-affine fractals and fractal dimension. Physica Scripta 32, 257–260.
Matthews, P.E., Bond, R.A.B., Van Den Berg, J.J., 1974. An algebraic method of strain analysis using elliptical markers. Tectonophysics 24, 31–67.
Marret, R., Allmendiger, R., 1991. Estimates of strain due to a brittle faulting: sampling of fault populations. Journal of Structural Geology 13, 735–738.
Marret, R., Allmendiger, R., 1992. Amount of extension on "small" faults: an example of from the Viking Graven. Geology 20, 47–50.
McNaught, M., 1994. Modifying the Normalized Fry Method for aggregates of non-elliptical grains. Journal of Structural Geology 16, 493–503.
Meere, P.A., Mulchrone, K.F., 2003. The effect of sample size on geological strain estimation from passively deformed clastic sedimentary rocks. Journal of Structural Geology 25, 1587–1595.
Meere, P.A., Mulchrone, K.F., Sears, J.W., Bradway, M.D., 2008. The effect of non-passive clast behaviour in the estimation of finite strain in sedimentary rocks. Journal of Structural Geology 30, 1264–1271.
Mulchrone, K.F., 2002. Application of Delaunay triangulation to the nearest neighbour method of strain analysis. Journal of Structural Geology 25, 689–702.
Mulchrone, K.F., 2005. An analytical error for the mean radial length method of strain analysis. Journal of Structural Geology 27, 1658–1665.
Mulchrone, K.F., Meere, P.A., 2001. A Windows program for the analysis of tectonic strain using deformed elliptical markers. Computers and Geosciences 27, 1253–1257.
Mulchrone, K.F., Meere, P.A., Roy Choudhury, K., 2005. SAPE: a program for semi-automatic parameter extraction for strain analysis. Journal of Structural Geology 27 (11), 2084–2098.
Mulchrone, K.F., O'Sullivan, F., Meere, P.A., 2003. Finite strain estimation using the mean radial length of elliptical objects with confidence intervals. Journal of Structural Geology 25, 529–539.
Pastor-Galán, D., 2008. Análisis de deformación finita en cinturones de pliegues y cabalgamientos (Talas Ala Tau, Kirguistán y Zona Cantábrica, NW de Iberia). Trabajo de Grado (M.Sc. thesis), University of Salamanca, Unpublished.
Pastor-Galán, D., Gutiérrez-Alonso, G., Mulchrone, K.F., Meere, P.A., 2008a. Análisis de deformación finita en el Antiforme del Narcea y el Manto de Somiedo, NO de España. Geo-Temas 10, 135.
Pastor-Galán, D., Gutiérrez-Alonso, G., Mulchrone, K.F., Meere, P.A., 2008b. Determinación de la deformación finita en dos secciones distintas (Talas Ala Tau, Kirguistán y Zona Cantábrica, NO de eespaña). Relaciones entre litología y deformación interna. Studia Geologica Salmanticensia 44 (2), 221–258.
Peach, C.J., Lisle, R.J., 1979. A Fortran IV program for the analysis of tectonic strain using deformed elliptical markers. Computers and Geosciences 5, 325–334.
Ramsay, J.G., 1967. Folding and Fracturing of Rocks. McGraw-Hill, New York.
Robin, P.F., 1977. Determination of geologic strain using randomly oriented strain markers of any shape. Tectonophysics 42, T7–T16.
Shimamoto, T., Ikeda, Y., 1976. A simple algebraic method for strain estimation from deformed ellipsoidal objects. 1. Basic theory. Tectonophysics 36, 315–337.
Turcotte, D.L., 1992. Fractals and Chaos in Geology and Geophysics. Cambridge University Press, Cambridge, p. 221.
Treagus, S.H., Treagus, J.E., 2002. Studies of strain and rheology of conglomerates. Journal of Structural Geology 24, 1541–1567.
Vitale, S., Mazzoli, S., 2005. Influence of object concentration on finite strain and effective viscosity contrast: insights from naturally deformed packstones. Journal of Structural Geology 27, 2135–2149.
Voitenko, V., Khudoley, A., Gertner, I., 2004. Influence of strain on the chemical composition of low-grade metamorphic sandstones: example from Talass Ala Tau, Kyrgyzstan. GeoLines 17, 100–101.
Weil, A.B., van der Voo, R., van der Pluijm, B.A., 2001. Oroclinal bending and evidence against the Pangea megashear: the Cantabria–Asturias arc (northern Spain). Geology 29 (11), 991–994.
Weil, A.B., Van der Voo, R., van der Pluijm, B.A., Pares, J.M., 2000. The formation of an orocline by multiphase deformation: a paleomagnetic investigation of the Cantabria–Asturias arc (northern Spain). Journal of Structural Geology 22 (6), 735–756.
Wu, S., 1993. Fractal strain distribution and its implication for cross-section balancing. Journal of Structural Geology 15, 1497–1507.
Yu, H., Zheng, Y., 1984. A statistical analysis applied to the $R_f/Ø$ method. Tectonophysics 110, 151–155.